Supporting Information for:

Triazenide-supported [Cu_4S] structural mimics of Cu_Z that mediate N_2O disproportionation rather than reduction

Neal P. Mankad
npm@uic.edu

Table of Contents:

GENERAL CONSIDERATIONS

Synthesis. Synthetic procedures were carried out under N_2 atmosphere inside a MBraun LabMaster glovebox or using standard Schlenk line techniques.[1] Reaction solvents were purified of air and moisture using a Glass Contours solvent purification system[2] built by Pure Process Technology, LLC, and stored over 3-Å molecular sieves in the glovebox. Deuterated solvents were degassed and then dried over 3-Å molecular sieves. The precursor compound, $Cu_2(NNN)_2$, was prepared according to literature procedures.[3] All other reagents were purchased from commercial vendors and used without further purification unless otherwise stated.

Instrumentation. ^{1}H NMR spectra were recorded using a Bruker Avance DPX-400-MHz spectrometer, with chemical shifts referenced using residual solvent peaks, and plotted in MestReNova. IR spectra were recorded on solid samples using a Bruker ALPHA spectrometer with a diamond-ATR detection unit. UV-Vis-NIR data were obtained using an Ocean Optics HDX-XR spectrometer fitted with a transmission dip probe and plotted in Origin after applying Lowess smoothing; peaks positions were determined by deconvolution as implemented in Origin. Cyclic voltammetry data was collected using a WaveNow USB Potentiostat from Pine Research Instrumentation using a classic three-electrode system[4] (glassy carbon working, Pt counter, $Ag/AgNO_3$ reference) and referenced to external $FeCp_2$. High-resolution EI mass spectra were recorded at the Mass Spectrometry Laboratory at the University of Illinois Urbana-Champaign using a Q-TOF MS instrument. X-band EPR spectra were recorded at 9.463473 GHz using a Bruker EMX EPR spectrometer and simulated using EasySpin.[5] Elemental analysis data were obtained by Atlantic Microlab, Inc. X-ray diffraction data for $\mathbf{1}^{\mathbf{N}}$ was collected at the X-ray diffraction facility at Cornell University using a Rigaku XtaLAB Synergy diffractometer, and for $[\mathbf{1}^{\mathbf{N}}][K(Krypt_{222})]$ at UIC using a Bruker D8 QUEST ECO diffractometer. Solution and refinement were done using the SHELX and OLEX2 software suites by standard methods.[6,7] Crystallographic data is available in CIF format by download from the CCDC (deposition numbers 2299540-2299541).

Computations. All DFT and TD-DFT calculations were performed using Gaussian16 (Revision B.01).[8] Geometries were optimized with no symmetry constraints using the B3LYP functional with ultrafine integration grid.[9,10] All atoms were treated using the def2TZVPP basis set.[11] Implicit solvation effects were included using the CPCM solvation model with default dichloromethane parameters.[12] Vibrational frequency analysis confirmed that all stationary points were correctly identified as either energy minima (zero imaginary frequencies) or saddle points (1 imaginary frequency). Transition states were further analyzed using implicit reaction coordinate scans along the imaginary frequency vector to verify that they were situated between reactant and product states on the potential energy surface. Mulliken population analysis was used to determine spin densities and molecular orbital coefficients. Reaction thermochemistry was calculated by including zero-point and thermal corrections to enthalpies and Gibbs free energies as implemented using default settings for vibrational frequency analysis in Gaussian16. Calculated UV-Vis-NIR spectra were generated in Gaussview using excited states calculated by TD-DFT after applying line broadening to qualitatively match experimental data. Coordinates for all relevant energy minima and saddle points are provided in XYZ format as Supporting Information attached to this manuscript.

For **TS2**, unfortunately, the geometry was not optimized at the level of theory indicated above after repeated attempts. Instead, the geometry could only be optimized successfully to the point of having exactly 1 imaginary frequency only in the gas phase (i.e, no CPCM solvation correction). Thus, although bond metrics for **TS2** are presented in the paper, reaction thermochemistry (i.e., activation energy) is omitted for this particular transition state.

SYNTHESIS & CHARACTERIZATION OF 1^N

Synthesis of $Cu_4(\mu_4\text{-}S)(NNN)_4$ (1^N). A solution of S_8 (10.7 mg, 0.0417 mmol) in toluene (2 mL) was added dropwise to a stirring solution of $Cu_2(NNN)_2$ (437 mg, 0.636 mmol) in THF (4 mL), causing an immediate color change from yellow to inky blue. After stirring the reaction overnight, volatiles were removed *in vacuo*. CH_3CN (3 mL) was added to the residue, and the resulting blue solid was collected by filtration and washed with additional CH_3CN (2 x 3 mL) followed by Et_2O (2 x 3 mL). Yield: 389 mg, 0.276 mmol, 87%. X-ray quality crystals spontaneously precipitated during removal of the THF/toluene reaction solvent. In both solution and solid state, the compound was found to be air stable indefinitely.

^1H NMR ($CDCl_3$, δ): 6.81 (1H), 6.74 (1H), 6.68 (1H), 6.34 (1H), 6.32 (1H), 2.59 (3H), 2.49 (3H), 2.36 (3H), 2.28 (3H), 2.22 (6H, overlapping singlets), 1.47 (3H), 1.32 (3H), 1.25 (3H). IR (solid, cm^{-1}): 2977, 2910, 2853, 1476, 1322, 1196, 883, 850. UV-Vis-NIR (CH_2Cl_2, λ_{max}): 602 (12000 $M^{-1}cm^{-1}$). Anal. calcd. for $C_{72}H_{88}Cu_4N_{12}S$: C, 61.43; H, 6.30; N, 11.94. Found: C, 61.70; H, 6.27; N, 11.81.

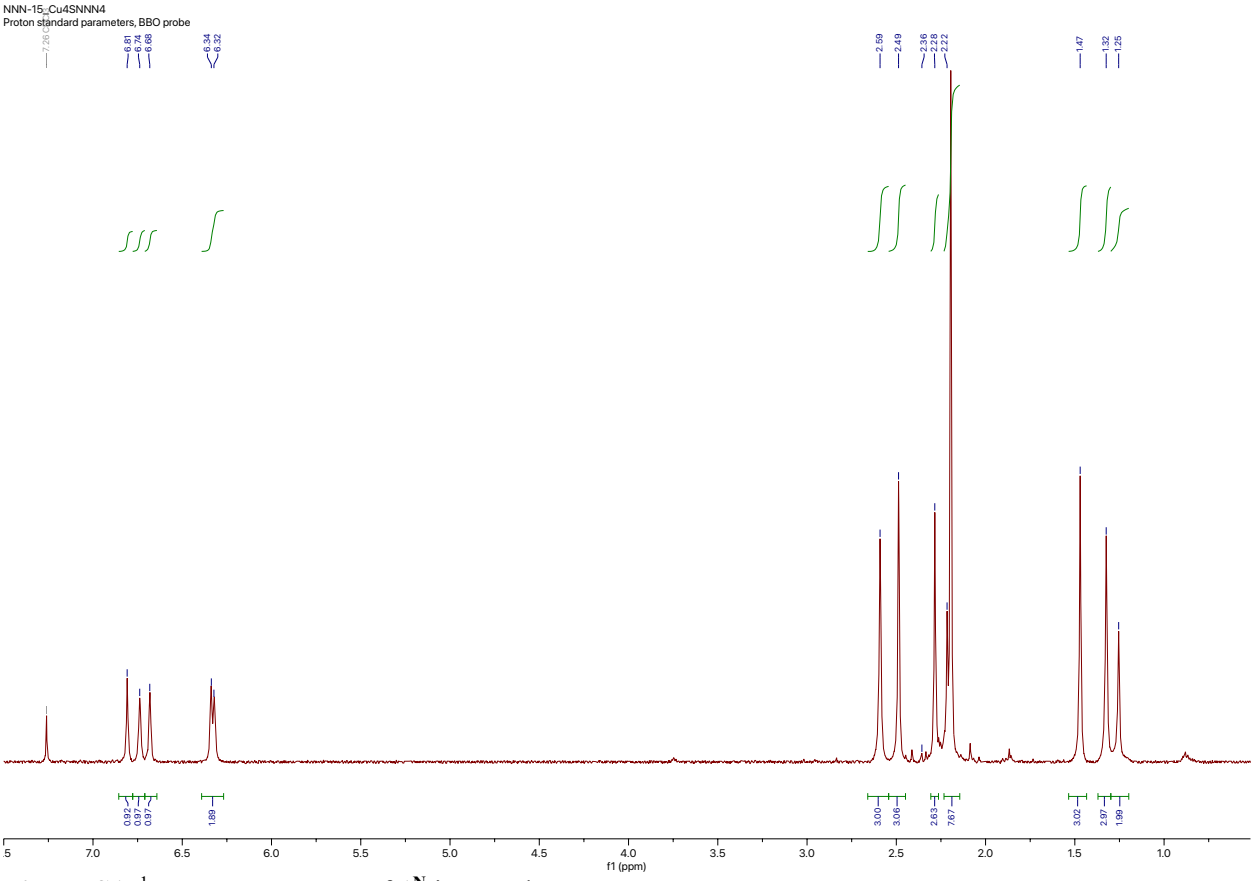

Figure S1. ^1H NMR spectrum of $\mathbf{1^N}$ in $CDCl_3$.

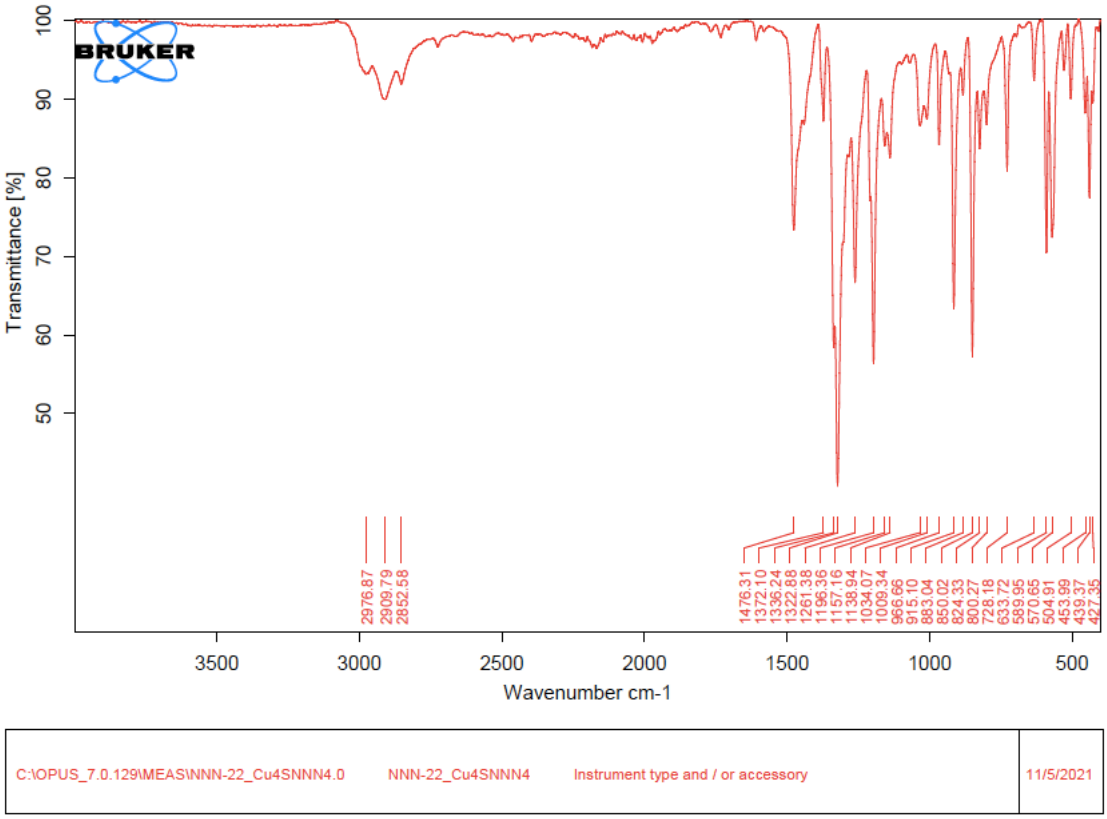

Figure S2. IR spectrum of $\mathbf{1}^{\mathbf{N}}$ in the solid state.

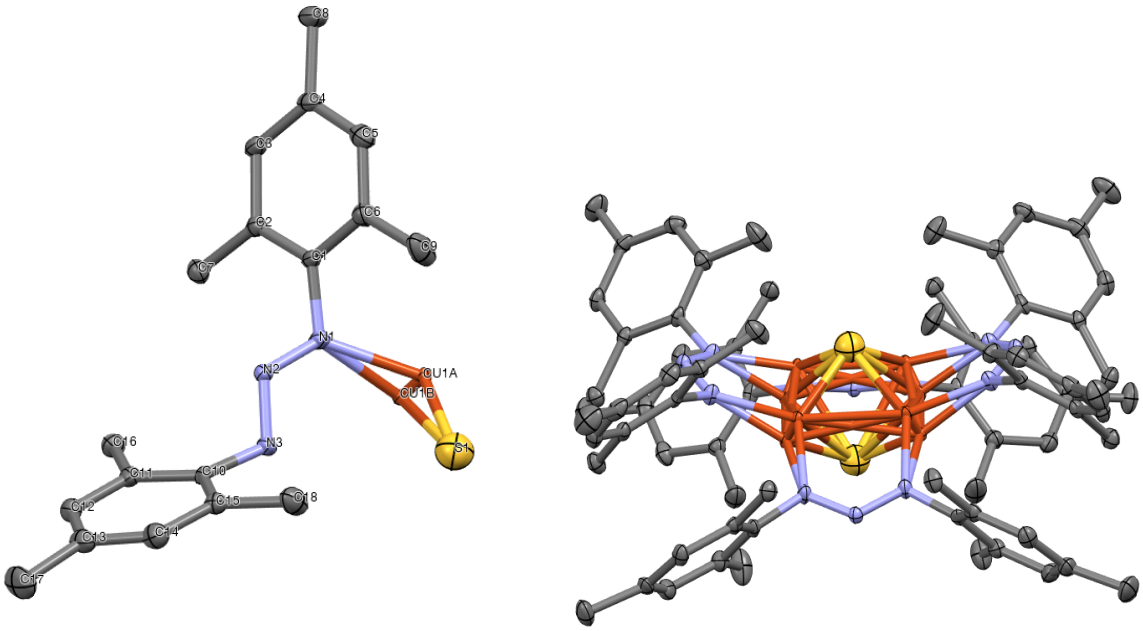

Figure S3. X-ray crystallography data for $\mathbf{1}^{\mathbf{N}}$: asymmetric unit (*left*) and molecular structure including all disordered components (*right*).

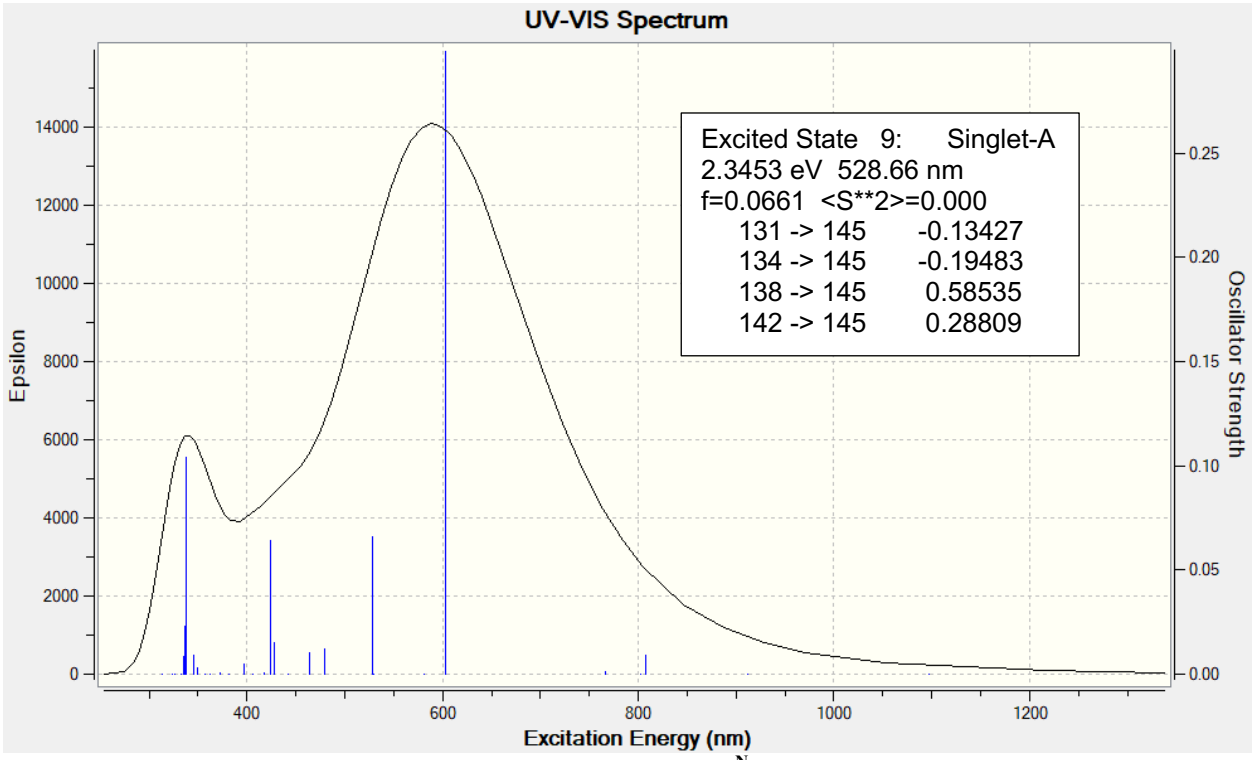

Figure S4. Calculated (TD-DFT) UV-Vis-NIR spectrum for $\mathbf{1}^{N}$ output by Gaussview, along with excitations comprising the main charge transfer state.

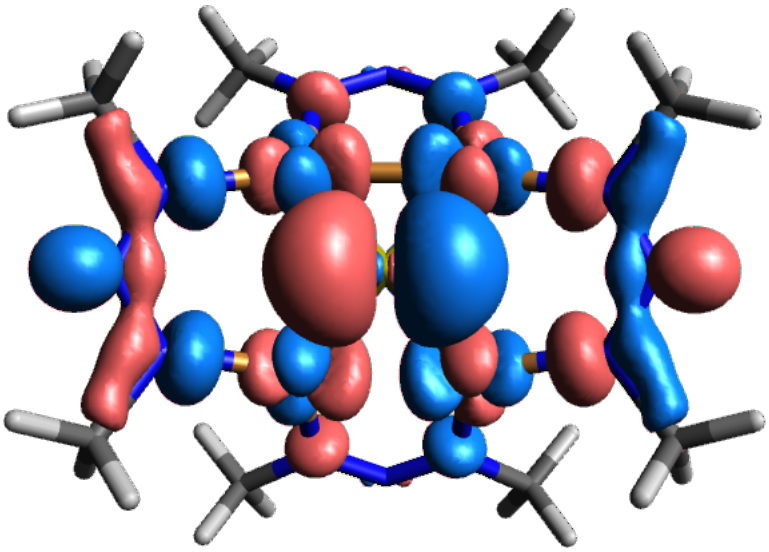

Figure S5. MO145 for $\mathbf{1}^{N}$, which is the acceptor orbital for all transitions admixed in excited state 9. Key orbital coefficients are given in the main text, Table 1.

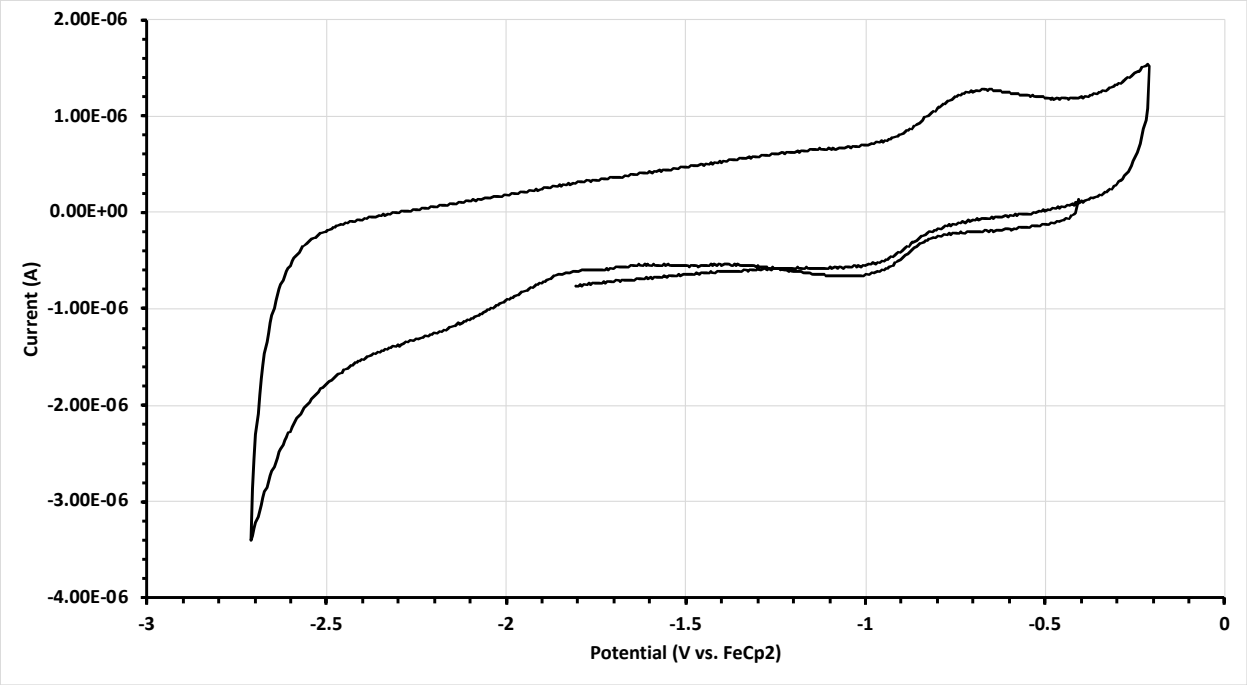

Figure S6. Cyclic voltammogram of $\mathbf{1^N}$ (2 mM) in THF with [nBu$_4$N][PF$_6$] supporting electrolyte (0.3 M). Initial potential was -0.4 V and scanning started in negative potential direction.

SYNTHESIS & CHARACTERIZATION OF [1^N][K(Krypt$_{222}$]

Synthesis of [$Cu_4(\mu_4$-S)$(NNN)_4$][K(Krypt$_{222}$)] ([$\mathbf{1^N}$][K(Krypt$_{222}$])). An orange solution of K[$FeCp(CO)_2$] (15.9 mg, 0.0736 mmol) in THF (2 mL) was added dropwise to a stirring blue suspension of $\mathbf{1^N}$ (99.5 mg, 0.0707 mmol) in THF (1 mL) at room temperature. Upon addition, the initial color was blue-green. A solution of Kryptofix-222 (28.1 mg, 0.0746 mmol) in THF (1 mL) was then added. The resulting solution was stirred for 1 h, over which time the color intensified to black. Volatiles were removed *in vacuo*. Toluene (3 mL) was added, and the resulting suspension was stirred for 5 min. Resulting solids were collected by filtration and washed with additional toluene (3 mL) and Et_2O (2 x 3 mL). The filtrate started red and became colorless during these washes, indicating complete removal of $[FeCp(CO)_2]_2$. The desired product was isolated as a blue powder. Yield: 102 mg, 0.0559 mmol, 79%. X-ray quality crystals were grown by slow diffusion of hexane vapors into a concentrated THF solution.

^{1}H NMR (acetone-d_6, δ): 3.62-3.58 (2H, overlapping singlets), 2.58 (1H). IR (solid, cm^{-1}): 2906, 1475, 1320, 1204, 1103, 945, 846, 850. UV-Vis-NIR (CH_2Cl_2, λ_{max}): 620 (4100 M^{-1}cm^{-1}), 934 (3300 M^{-1}cm^{-1}). EPR (X-band, 1:1 CH_3CN:CH_2Cl_2): g_{iso} = 2.071. Anal. calcd. for $C_{90}H_{124}Cu_4KN_{14}O_6S$: C, 59.28; H, 6.85; N, 10.75. Found: C, 58.21; H, 6.73; N, 10.35.

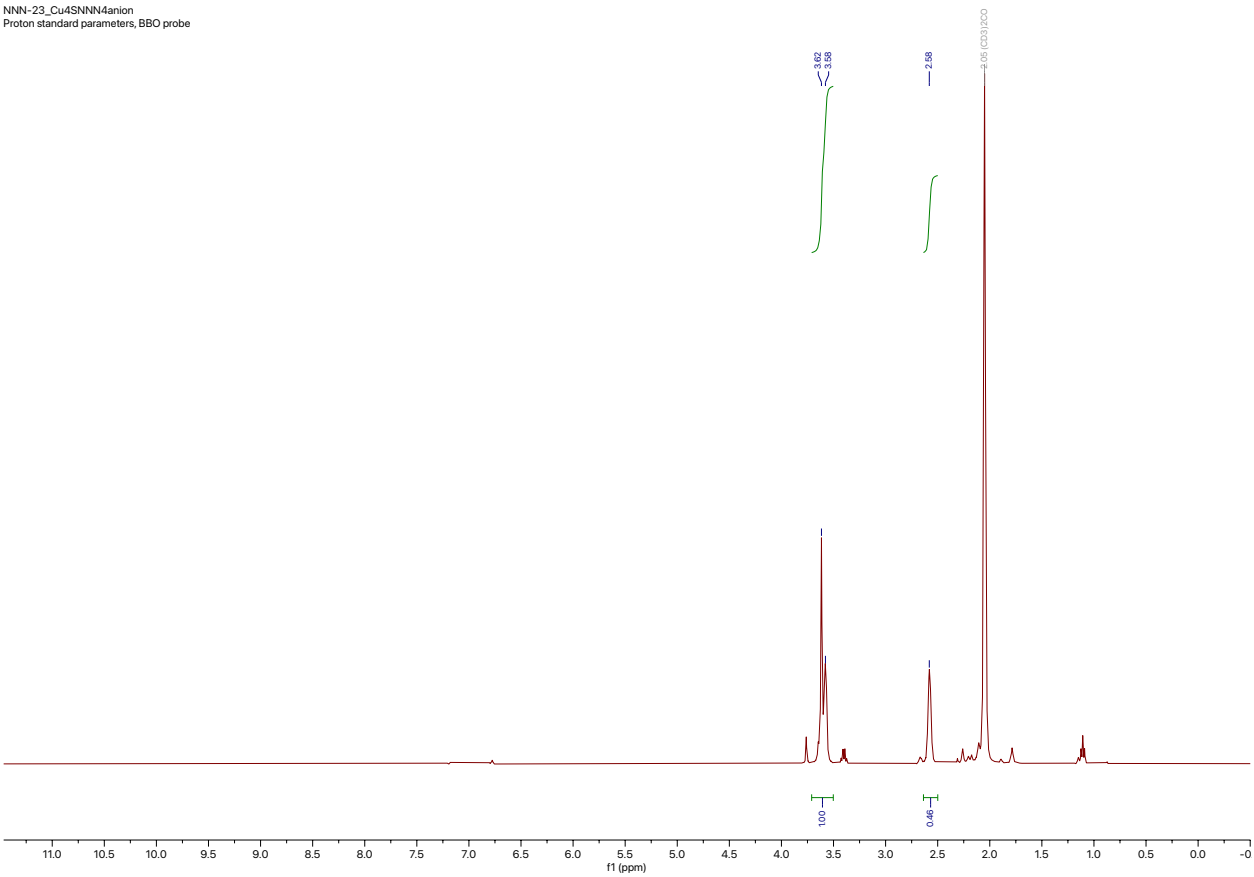

Figure S7. ^{1}H NMR spectrum of [$\mathbf{1^N}$][K(Krypt$_{222}$)] in acetone-d_6.

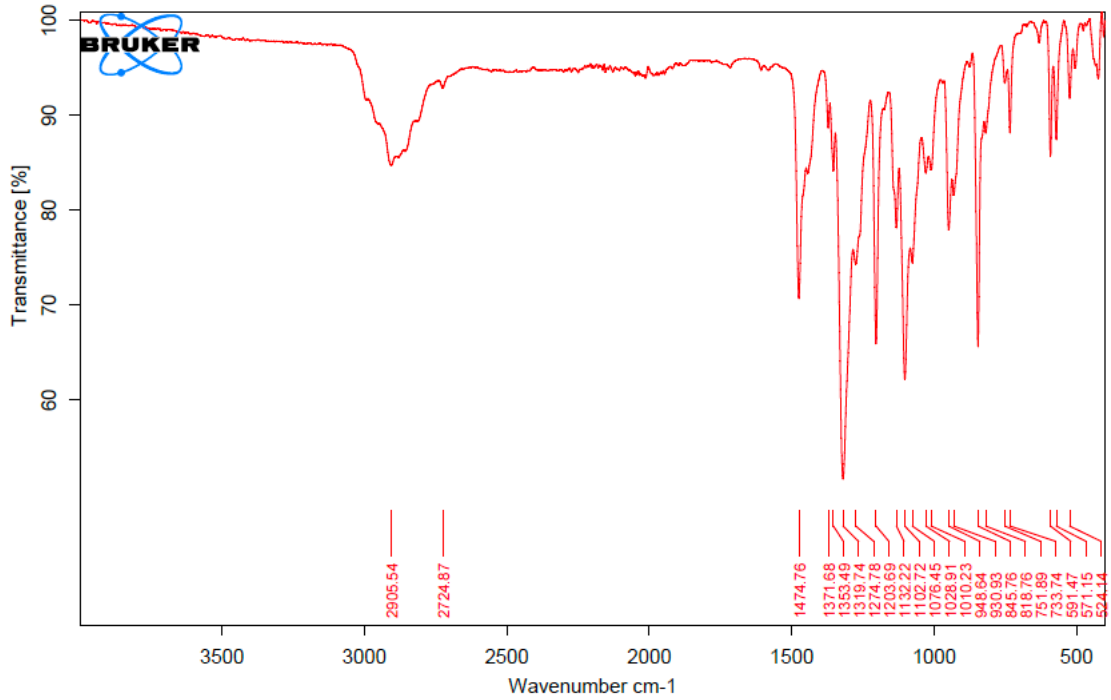

Figure S8. IR spectrum of [$\mathbf{1}^{N}$][K(Krypt$_{222}$)] in the solid state.

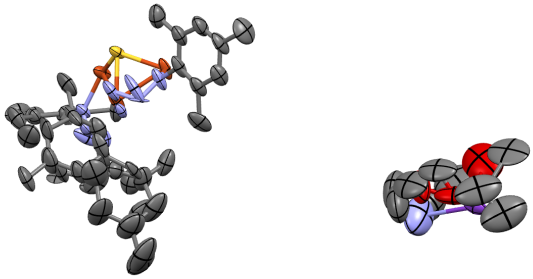

Figure S9. X-ray crystallography data: asymmetric unit for [$\mathbf{1}^{N}$][K(Krypt$_{222}$)].

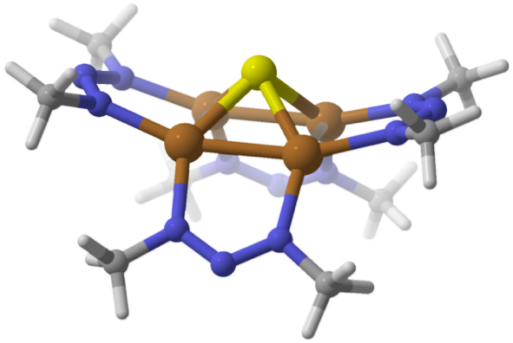

Figure S10. Optimized geometry for the DFT model of [$\mathbf{1}^{N}$]$^{-}$

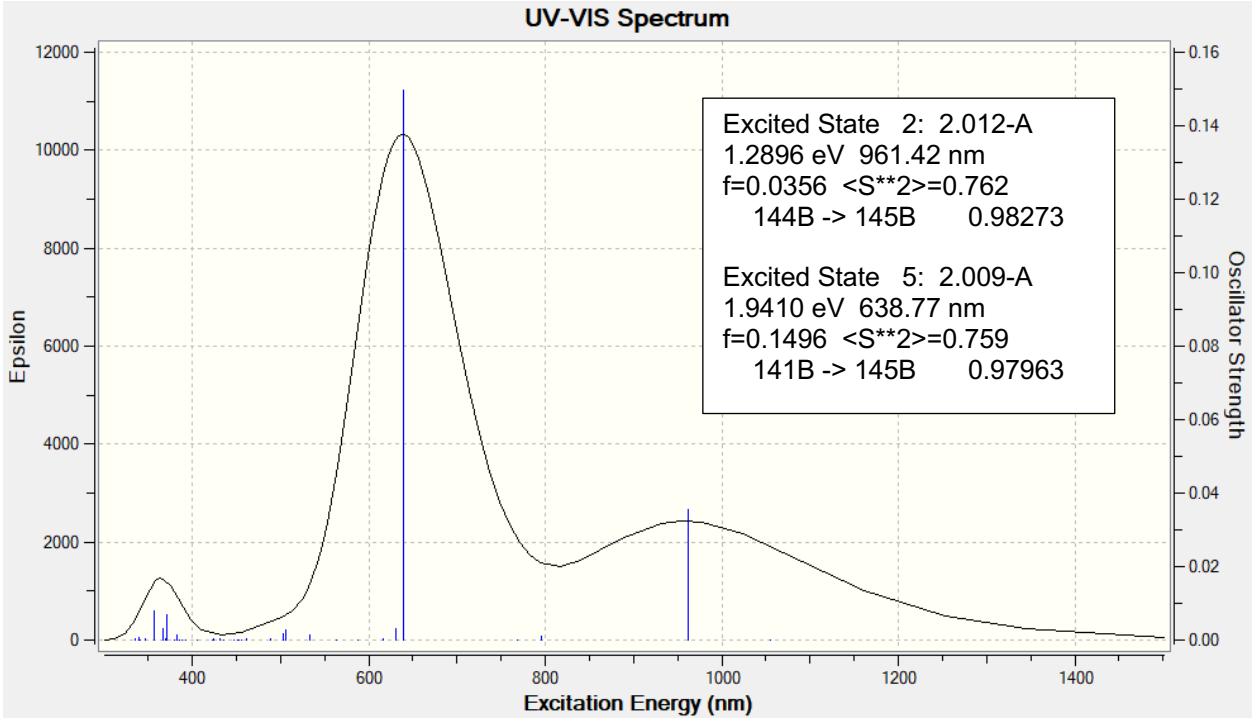

Figure S11. Calculated (TD-DFT) UV-Vis-NIR spectrum for $[\mathbf{1}^{N}]^{-}$ output by Gaussview, along with excitations comprising the two main charge transfer states.

N_2O REACTIVITY

Reaction with N_2O gas. A representative procedure is given here from among the various conditions that were examined. CH_2Cl_2 (6 mL) was added to [**1**^{N}][K(Krypt$_{222}$)] (96.5 mg, 0.0529 mmol) and $CoCp_2$ (12.8 mg, 0.0677 mmol) in a Schlenk tube with a magnetic stir bar. The solution was degassed by three freeze-pump-thaw cycles, the flask was backfilled with N_2O (1 atm), and then the reaction was stirred vigorously overnight. Over this time, the solution gradually darkened its blue color. The reaction mixture was filtered through a Celite pad to remove some dark-colored precipitate. After washing the Celite pad with additional CH_2Cl_2 (2 x 3 mL), the filtrate was concentrated *in vacuo*. The residue was washed with pentane (3 x 3 mL), removing a light orange supernatant each time. A 5:1 mixture of Et_2O/toluene (10 mL) was added to the solid residue. After trituration, the solution was filtered into a tared vial. Volatiles were removed *in vacuo* to yield a brown solid. Yield: 9.5 mg, 0.0067 mmol, 13%. ^{1}H NMR analysis of this solid revealed **2** with some small impurities including Krypt$_{222}$ and trace **1**^{N}. Analysis of the solid by UV-Vis-NIR and HRMS provided the data shown in the main manuscript (Figure 3a). The remaining, insoluble materials from the combined previous filtrations were diluted with THF and analyzed by UV-Vis-NIR, showing that the major species is unreacted [**1**^{N}][K(Krypt$_{222}$)].

^{1}H NMR for **2** ($CDCl_3$, δ): 6.81 (2H), 2.28 (6H), 2.21 (3H).

Reaction with Me_3NO. A representative procedure is given here from among the various conditions that were examined. A solution of $CoCp_2$ (32.5 mg, 0.172 mmol) in CH_2Cl_2 (2 mL) was added to a suspension of **1**^{N} (109.6 mg, 0.0779 mmol) in CH_2Cl_2 (3 mL). Immediately, the reaction color changed from inky blue to dull blue with formation of a small amount of precipitate. After 5 min, a solution of Me_3NO (8.2 mg, 0.11 mmol) in CH_2Cl_2 (2 mL) was added. The reaction was allowed to stand overnight, after which the reaction mixture had become cloudy and brown in color. An aliquot was dried *in vacuo*, reconstituted in $CDCl_3$, and analyzed by ^{1}H NMR, revealing predominantly a mixture of **2**, $[CoCp_2]^+$ (presumably paired with [**1**^{N}]$^-$), and Me_3NO (see figure below). For the remainder of the reaction mixture, volatiles were removed *in vacuo*, and toluene (5 mL) was added. After filtration, a yellow-brown filtrate and blue solid were obtained. Analysis of the solid by ^{1}H NMR and UV-Vis-NIR indicated a mixture of **1**^{N} and [**1**^{N}][$CoCp_2$]. The filtrate was concentrated *in vacuo*. The residue was washed with pentane (3 x 3 mL) and dried *in vacuo*. The remaining trace solid (est. < 5 mg) was dissolved in $CDCl_3$ and analyzed by ^{1}H NMR, revealing a relatively pure sample of **2** (albeit with trace impurities, see figure below).

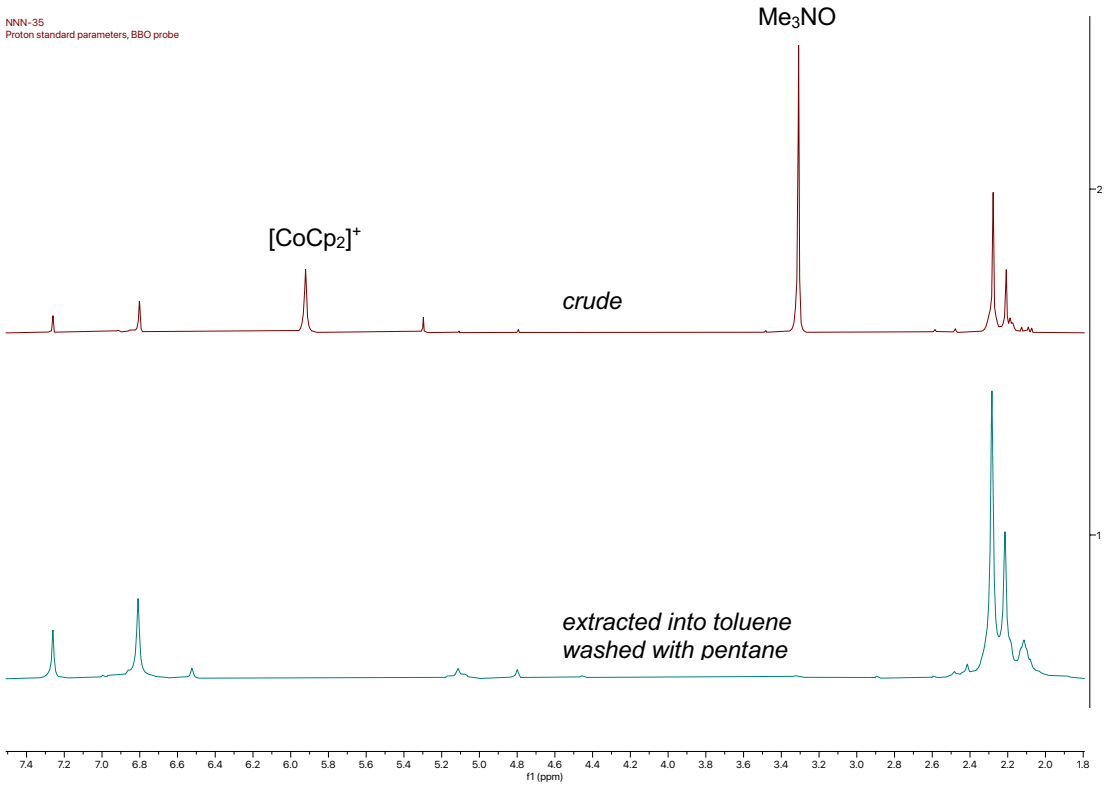

Figure S12. Representative NMR data from O-atom transfer experiments: crude mixture from Me_3NO experiment (*top*) and toluene-soluble fraction after washing with pentane (*bottom*).

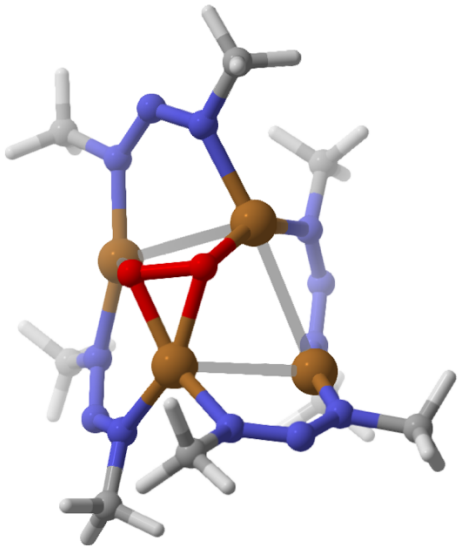

Figure S13. An alternative O_2 binding mode calculated to be 13.6 kcal/mol higher in energy than the structure of **2** presented in the main manuscript.

REFERENCES

(1) Borys, A. M. An Illustrated Guide to Schlenk Line Techniques. *Organometallics* **2023**, *42* (3), 182–196. https://doi.org/10.1021/acs.organomet.2c00535.
(2) Pangborn, A. B.; Giardello, M. A.; Grubbs, R. H.; Rosen, R. K.; Timmers, F. J. Safe and Convenient Procedure for Solvent Purification. *Organometallics* **1996**, *15* (5), 1518–1520. https://doi.org/10.1021/om9503712.
(3) Alayoglu, P.; Chang, T.; Lorenzo Ocampo, M. V.; Murray, L. J.; Chen, Y.-S.; Mankad, N. P. Metal Site-Specific Electrostatic Field Effects on a Tricopper(I) Cluster Probed by Resonant Diffraction Anomalous Fine Structure (DAFS). *Inorg. Chem.* **2023**, *62* (37), 15267–15276. https://doi.org/10.1021/acs.inorgchem.3c02472.
(4) Elgrishi, N.; Rountree, K. J.; McCarthy, B. D.; Rountree, E. S.; Eisenhart, T. T.; Dempsey, J. L. A Practical Beginner's Guide to Cyclic Voltammetry. *J. Chem. Educ.* **2018**, *95* (2), 197–206. https://doi.org/10.1021/acs.jchemed.7b00361.
(5) Stoll, S.; Schweiger, A. EasySpin, a Comprehensive Software Package for Spectral Simulation and Analysis in EPR. *J. Magn. Reson.* **2006**, *178* (1), 42–55. https://doi.org/10.1016/j.jmr.2005.08.013.
(6) Dolomanov, O. V.; Bourhis, L. J.; Gildea, R. J.; Howard, J. a. K.; Puschmann, H. OLEX2: A Complete Structure Solution, Refinement and Analysis Program. *J. Appl. Crystallogr.* **2009**, *42* (2), 339–341. https://doi.org/10.1107/S0021889808042726.
(7) Sheldrick, G. M. A Short History of SHELX. *Acta Crystallogr. A* **2008**, *64* (1), 112–122. https://doi.org/10.1107/S0108767307043930.
(8) Ortiz, J. V.; Cioslowski, J.; Fox, D. J. Gaussian 09, Revision B. 01. *Wallingford CT* **2009**.
(9) Becke, A. D. Density-functional Thermochemistry. III. The Role of Exact Exchange. *J. Chem. Phys.* **1993**, *98* (7), 5648–5652. https://doi.org/10.1063/1.464913.
(10) Lee, C.; Yang, W.; Parr, R. G. Development of the Colle-Salvetti Correlation-Energy Formula into a Functional of the Electron Density. *Phys. Rev. B* **1988**, *37* (2), 785.
(11) Zheng, J.; Xu, X.; Truhlar, D. G. Minimally Augmented Karlsruhe Basis Sets. *Theor. Chem. Acc.* **2011**, *128* (3), 295–305. https://doi.org/10.1007/s00214-010-0846-z.
(12) Cossi, M.; Rega, N.; Scalmani, G.; Barone, V. Energies, Structures, and Electronic Properties of Molecules in Solution with the C-PCM Solvation Model. *J. Comput. Chem.* **2003**, *24* (6), 669–681. https://doi.org/10.1002/jcc.10189.